THE JOURNAL OF COMPARATIVE NEUROLOGY 458:334–349 (2003)

Not All Butterfly Eyes Are Created Equal: Rhodopsin Absorption Spectra, Molecular Identification, and Localization of Ultraviolet-, Blue-, and Green-Sensitive Rhodopsin-Encoding mRNAs in the Retina of *Vanessa cardui*

ADRIANA D. BRISCOE,[1]* GARY D. BERNARD,[2] ALLAN S. SZETO,[3] LISA M. NAGY,[3] AND RICHARD H. WHITE[4]

[1]Department of Ecology and Evolutionary Biology, University of California, Irvine, California 92697

[2]Department of Electrical Engineering, University of Washington, Seattle, Washington 98195

[3]Department of Molecular and Cellular Biology, University of Arizona, Tucson, Arizona 85721

[4]Department of Biology, University of Massachusetts, Boston, Massachusetts 02125

ABSTRACT

Surveys of spectral sensitivities, visual pigment spectra, and opsin gene sequences have indicated that all butterfly eyes contain ultraviolet-, blue-, and green-sensitive rhodopsins. Some species also contain a fourth or fifth type, related in amino acid sequence to green-sensitive insect rhodopsins, but red shifted in absorbance. By combining electron microscopy, epi-microspectrophotometry, and polymerase chain reaction cloning, we found that the compound eye of *Vanessa cardui* has the typical ultrastructural features of the butterfly retina but contains only the three common insect rhodopsins. We estimated lambda-max values and relative densities of the rhodopsins in the *Vanessa* retina (0.72, P530; 0.12, P470; and 0.15, P360) from microspectrophotometric measurements and calculations based on a computational model of reflectance spectra. We isolated three opsin-encoding cDNA fragments that were identified with P530, P470, and P360 by homology to the well-characterized insect rhodopsin families. The retinal mosaic was mapped by opsin mRNA in situ hybridization and found to contain three kinds of ommatidia with respect to their patterns of short wavelength rhodopsin expression. In some ommatidia, P360 or P470 was expressed in R1 and R2 opposed receptor cells; in others, one cell expressed P360, whereas its complement expressed P470. P530 was expressed in the other seven cells of all ommatidia. P470-expressing cells were abundant in the ventral retina but nearly absent dorsally. Our results indicated that there are major differences between the color vision systems of nymphalid and papilionid butterflies: the nymphalid *Vanessa* has a simpler, trichromatic, system than do the tetrachromatic papilionids that have been studied. J. Comp. Neurol. 458:334–349, 2003.

Indexing terms: color vision; photoreceptor; visual pigment; Nymphalidae; Lepidoptera

Grant sponsor: National Science Foundation; Grant number: IBN-9874624 (L.M.N.); Grant number: IBN-0082700 (A.D.B and S.B.); Grant number: IBN-9874493 (R.H.W).

*Correspondence to: Adriana D. Briscoe, Department of Ecology and Evolutionary Biology, University of California, Irvine, 321 Steinhaus Hall, Irvine, CA 92697. E-mail: abriscoe@uci.edu

Received 11 July 2002; Revised 4 September 2002; Accepted 22 November 2002

DOI 10.1002/cne.10582

Published online the week of February 24, 2003 in Wiley InterScience (www.interscience.wiley.com).

Butterflies use visual cues for a variety of behaviors: foraging (Weiss, 2001), host plant identification (Kelber, 1999), territoriality of males (Bernard and Remington, 1991), and mate recognition (Silberglied, 1989; Jiggins et al., 2001). Despite sharing these basic life history traits, large behavioral differences mediated in part by vision have long been documented among families of butterflies. For instance, Ilse (1965) reported that pierid and papilionid butterflies could distinguish violet from purple and dark red, and nymphalid butterflies were particularly adept at discriminating light from dark. The extent to which these differences in chromatic and achromatic vision may be driven by variations in the organization and patterning of the retina is largely unknown. Although all butterfly families appear to be invariant in the number of photoreceptor cells (nine) per ommatidium (Gordon, 1977; Shimohigashi and Tominaga, 1986), differences have been documented in the number and peak sensitivity of spectral classes of photoreceptor (reviewed in Briscoe and Chittka, 2001), the number and distribution of filtering pigments present (Ribi, 1978; Arikawa and Stavenga, 1997; Arikawa et al., 1999; Qiu et al., 2002), and the presence or absence of accessory optical structures such as the tapetum (Miller and Bernard, 1968; Ribi, 1979).

In butterflies that exhibit eyeshine reflected from ommatidial tapeta (Miller and Bernard, 1968; Ribi, 1979; Stavenga et al., 2000, 2001), it is possible to use an epi-illumination microscope to measure absorption spectra of rhodopsin in the eye of a completely intact butterfly (Bernard, 1981, 1983a,b). This is possible because the visual pigment cycle of butterflies is unusual among the invertebrates; the metarhodopsin photoproduct of rhodopsin is not stable in the dark but disappears from the rhabdom with first-order kinetics. The rhodopsin titer recovers in the dark but with multicomponent kinetics that are slower than those for decay of metarhodopsin. Consequently, it is possible to bleach the rhabdoms of a visual pigment by delivering a series of bright photoisomerizing flashes separated by dark periods. Work of this kind has shown that *Vanessa cardui* has P530 as the majority visual pigment (Bernard, 1983a), but has no visual pigments with a spectral position (λmax) greater than 530 nm, nor is there any evidence for colored lateral filters as described in some Pieridae and Papilionidae (Ribi, 1978; Arikawa and Stavenga, 1997). Electrophysiological experiments with *V. cardui* have shown that the eye also contains an ultraviolet (UV)–absorbing visual pigment absorbing maximally at 360 nm (Chen, 1987). Since most insects that have been adequately tested also have blue-sensitive classes of photoreceptor (Fig. 1 in Peitsch et al., 1992; Kinoshita et al., 1997), we examined the *Vanessa* retina for the presence of a blue rhodopsin. Using epi-microspectrophotometry, we estimated the λmax of the blue rhodopsin and the optical densities of all three visual pigments contained in the rhabdoms.

At the RNA level all Lepidoptera surveyed thus far have at least two transcripts that encode short wavelength (UV and blue)–sensitive rhodopsins (Chase et al., 1997; Briscoe, 1998; Kitamoto et al., 2000). In contrast, Lepidoptera appear to be heterogeneous in the number of long wavelength-sensitive (LWS) opsin genes they possess. Four LWS opsin cDNAs have been isolated from two species in the papilionid butterfly family (Briscoe, 1998, 1999, 2000; Kitamoto et al., 1998). More recent surveys of LWS opsin diversity have indicated that three of these LWS opsins are related by two gene duplication events, which occurred since the papilionid and nymphalid butterfly families shared a common ancestor (Briscoe, 2001; Hsu et al., 2001; Fig. 1). The spatial distribution of these three LWS opsin mRNAs in the retina of *Papilio* spp. is complex, with dorsal and ventral patterning differences and overlapping and nonoverlapping expressions in different subsets of R3 through R9 photoreceptor cells (Kitamoto et al., 1998, Briscoe and Nagy, unpublished observations). To examine whether a butterfly with one LWS retina-specific opsin (Briscoe, 2001) also has a simpler patterning of the eye with respect to the spatial distribution of visual pigments, we cloned and investigated the expression pattern of the UV-, blue- and green-sensitive rhodopsin-encoding mRNAs of *V. cardui* (Nymphalidae).[1] We found that the UV and blue rhodopsin-encoding mRNA expression patterns in individual photoreceptor cells are similar (but not identical) between nymphalid and papilionid butterflies, whereas the expression pattern of the green opsin is not. *Vanessa cardui* has a much simpler spatial distribution of opsin mRNAs in the retina than do *Papilio* spp. (Papilionidae).

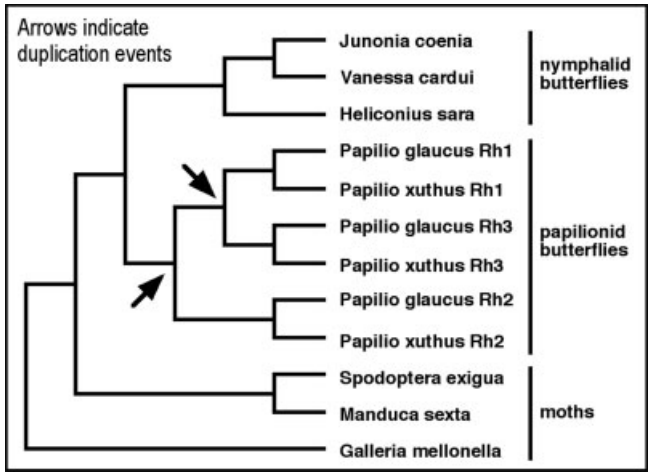

Fig. 1. Phylogeny of long wavelength-sensitive lepidopteran opsins simplified from Figure 3 of Briscoe (2001). Arrows indicate two gene duplication events along the papilionid lineage leading to additional green- (Rh1) and red- (Rh3) sensitive visual pigment transcripts expressed in the retina (Kitamoto et al., 1998). Branching pattern of opsins in the nymphalid clade mirrors known biological relationships between the species from which these sequences were sampled. The sequence from the most basal moth lineage represented, *Galleria mellonella* (Pyralidae), was used as an outgroup.

MATERIALS AND METHODS

Animals

Pupae of *V. cardui* were obtained from Carolina Biological Supply Co. (Burlington, NC) and allowed to eclose. Adults were fed honey water daily for 7 to 12 days until they were killed. Unless otherwise specified, the adult

[1]We refer to the transcripts encoding the UV-sensitive, blue-sensitive, green-sensitive rhodopsins as the *VanUV* mRNA, *VanB* mRNA, and *VanG* mRNAs, respectively.

butterflies were placed at 4°C for 1 hour before being killed by a swift severing of the body (with forceps) near the attachment of the wings to the thorax.

DNA and RNA isolation

Genomic DNA was extracted from the thorax and abdomen of four *Vanessa* adults according to the methods of Hsu et al. (2001). Total RNA also was extracted from two adult butterfly heads according to the Trizol extraction protocol (GibcoBRL, Gaithersburg, MD) and resuspended in diethyl pyrocarbonate–treated H_2O. With the total RNA extracted, a pool of cDNA was synthesized through reverse transcription with the use of an adaptor primer and Superscript Reverse Transcriptase (GibcoBRL).

Polymerase chain reaction, cloning, and sequencing

With cDNA as the template, a polymerase chain reaction (PCR) was run (for 1 minute at 94°C and then 35 cycles of 30 seconds at 94°C, 1 minute at 50°C, and 1 minute at 72°C) first with degenerate primer 80 (5′-GAA CAR GCW AAR AAR ATG A-3′) and then with Race2 (a primer complementary to the adaptor primer) to generate 3′RACE products. To detect multiple LWS opsins, if present, genomic DNA also was used as a template in a PCR with the primers 80-OPSRD (5′-CCR TAN ACR ATN GGR TTR TA-3′), which amplify a short intron-containing region of the long wavelength opsin gene (Briscoe, 1999). These same primers were sufficient to amplify multiple LWS opsins from *Papilio* genomic DNA detectable by differences in intron length and sequence (Briscoe, unpublished observation). After amplification, the PCR products were cloned (TOPO-TA Cloning Kit, Invitrogen, La Jolla, CA). The plasmids were amplified with M13Fd and M13Rd primers in a colony PCR, and the Concert Purification Kit (Invitrogen) was used to purify the PCR products for sequencing. The purified PCR product was then cycle sequenced with an ABI Prizm 377 DNA Sequencer with Dye Primer and Dye Terminator Cycle Sequencing Ready Reaction kits (Applied Biosystems, Foster City, CA).

Phylogenetic analysis

Amino acid sequences of 32 invertebrate opsins were downloaded from GenBank and aligned by using Clustal W (Thompson et al., 1994). The neighbor-joining algorithm was used to construct phylogenetic trees of the nucleotide sequences under several models of nucleotide evolution (Kimura 2-parameter, HKY85, general time reversible), with minimum evolution as the objective function. The two opsins from the crab *Hemigrapsus sanguineus* were used as outgroups. The robustness of the trees was evaluated with the bootstrap method as implemented in PAUP*.

GenBank accession numbers of sequences used in the phylogenetic analysis are as follows:

Apis mellifera (honeybee): UV, AF004169; blue, AF004168; LW, U26026
Camponotus abdominalis (carpenter ant): UV, AF042788; LW, U32502
Drosophila melanogaster (fruit fly): Rh1, K02315; Rh2, M12896; Rh3, M17718; Rh4, M17730; Rh5, U67905; Rh6, Z86118
Hemigrapsus sanguineus (crab): 1, D50583; 2, D50584
Limulus polyphemus (horseshoe crab): lateral eye, L03781; ocelli, L03782
Manduca sexta (moth): green, L78080; UV, L780801; blue, AD001674
Megoura viciae (aphid): UV, AF189715; LW, AF189714
Papilio glaucus (butterfly): PglRh1, AF077189; PglRh2, AF077190; PglRh3, AF067080; PglRh4, AF077193; PglRh5, AF077191; PglRh6, AF077192
Procambarus clarkii (crayfish): S53494
Schistocerca gregaria (locust): 1, X80071; 2, X80072
Sphodromantis spp. (mantid): X71665
Vanessa cardui (butterfly): UV, AF414074; blue, AF414075; green, AF385333

Epi-microspectrophotometry of intact eyes

Eyeshine created by multilayered tracheolar mirrors makes the eye of an intact butterfly an ideal preparation for spectroscopic study of visual pigments. Consider the optics. Visual pigments are contained within a long, thin rhabdom waveguide that is illuminated efficiently by a pair of lenses at one end (Nilsson et al., 1988) and terminated optically by an interference reflector at the other end. Light propagates down the rhabdom waveguide, being partly absorbed by visual pigments as it goes. The fraction of light that survives to exit the rhabdom is reflected at the tapetum and propagated back up the rhabdom, again being partly absorbed. Light that survives this double pass through the rhabdom is collected by the lenses and passes out of the eye, where it is observable as a narrow beam of eyeshine. Thus, the integrated longitudinal absorbance spectrum of the rhabdom is proportional to one-half the common logarithm of the reflectance spectrum that is measured by the epi-microspectrophotometer.

The experimental procedure was described by Bernard (1982, 1983a,b). Briefly, a completely intact *V. cardui* was mounted on the goniometer stage of a double-beam, epi-illumination microspectrophotometer, and the microscope objective was focused on the deep pseudopupil for optimal collection of eyeshine and reduction of stray light. When the thoroughly dark-adapted eye was illuminated with an intense orange flash, a substantial fraction of visual pigment P530 was photoisomerized, creating a metarhodopsin photoproduct, M490, which decays exponentially with time in the dark at a rate that depends strongly on temperature. Repeated flashes of bright orange light separated by dark periods greater than the decay time of M490 leaves the eye in a partly bleached state. The difference spectrum for this partial bleach directly yields the absorbance spectrum of P530.

When bright blue flashes are delivered to such an eye, the photochemistry of the blue-absorbing visual pigment can be studied. P470 photoconverts to a photoproduct, M500, whose absorbance spectrum is shifted to longer wavelengths. The difference spectra produced by blue flashes are small compared with measured difference spectra for R530 and M490, as if the maximal density of P470 was approximately one-fourth the density of P530. The kinetics for decay of M500 is faster than for recovery of P470, so it is possible with a series of flashes separated by dark periods to bleach the rhabdoms of P530 and P470. When bright UV flashes are delivered to the eye in this state, they photoconvert the UV-absorbing visual pigment to its M465 photoproduct. From the electrophysiological

work of Chen (1987), we know that the UV-absorbing visual pigment absorbs maximally at 360 nm.

In the detailed examples given by Bernard (1983a, Fig. 2; 1983b, Fig. 3b) rhabdoms of 20 ommatidia were bleached in this way, from the eye region that was at elevation 15 degrees below the center of the acute zone[2] and at azimuth 20 degrees from mid-line. The eyeshine reflectance spectrum for the eye in a substantially bleached state is shown in Figure 1B of Bernard (1983b). The basis for reduced reflectance for wavelengths shorter than 600 nm was that the rhabdoms were not entirely empty of P530 and contained other visual pigments. Similar experiments with this same individual butterfly were continued for 5 days. Near the end of that series, after having dark adapted the butterfly for 64 hours, it was fed honey water and allowed to view the blue sky for 30 minutes, remounted, then dark adapted for 2 hours at 75°F. Measurements of difference spectra during that time showed that all metarhodopsin M490 created by exposure to skylight had decayed from the rhabdoms by the end of the 2 hours, but the density of P530 had not fully recovered, being about 0.1 log-units shy of a full titer. The reflectance spectrum at the end of those 2 hours was measured.

By following the analytical procedure described by Bernard and Remington (1991) for lycaenid butterflies, it is possible to estimate quantitatively the visual pigment content of rhabdoms when the tapetal reflectance spectrum is constant (white) for wavelengths shorter than about 650 nm. To investigate whether this might also be true for *V. cardui*, we prepared electron micrographs of longitudinal sections of an individual tapetum. We computed a theoretical reflectance spectrum (Brekhovskikh, 1960) for a system of 80 planar multilayers of alternating high (1.5) and low (1.0) refractive indexes by using layer thicknesses measured from the electron micrographs. As discussed below, the computed reflectance is greater than 90% for wavelengths between 320 and 680 nm, thereby justifying the assumption of a white reflectance spectrum in that band. From this information, we created a computational model of the expected reflectance spectrum for mixed ommatidia and compared this spectrum with our measured reflectance spectrum. Details of this model are given in the Appendix.

Transmission electron microscopy

Light-adapted adult eyes were fixed for histology on the day of emergence. Heads were bisected into the cacodylate buffered glutaraldehyde-formaldehyde fixative (White and Bennett, 1989). After aldehyde fixation for 1.0 to 2.0 hours, the tissue was washed in buffer and postfixed in 0.5% OsO_4 for 1 hour. After a water rinse, the tissue was stained in 2% uranyl acetate in darkness for 1 to 2 hours. The tissue was dehydrated in ethanol and propylene oxide and embedded in Spurr's resin (Polysciences, Warrington, PA). Sections, 1 μm thick, were stained with methylene blue for light microscopy. Digital light micrographs were obtained with an Olympus BX60 microscope and Scionimage software. Thin sections were stained with lead citrate for electron microscopy. Electron micrographs were photographed in a Philips 300 electron microscope. Light and electron micrographs were processed in Adobe Photoshop 4.0, with only contrast and density adjusted for the preparation of Figure 6.

Opsin in situ hybridization

The eyes were fixed in 4% paraformaldehyde in 1× phosphate buffered saline (pH 7.2) for 1 to 2 hours and stepped through a sucrose gradient from 10% to 30%. Then the tissue was cryostat sectioned into 12- to 16-μm slices, or the ommatidia were manually dissociated, placed onto slides, and stored at −20°C. Starting with 400 ng of purified PCR product (amplified from plasmid DNA), RNA probes (riboprobes) complementary to the mRNAs of the visual pigments were synthesized with digoxigenin-labeled UTPs by using a Boehringer Mannheim Genius Kit (Boehringer Mannheim, Indianapolis, IN). As a control for the specificity of opsin mRNA expression, sense-strand riboprobes were also synthesized for each of the three cDNAs (*VanUV*, *VanB*, and *VanG*). The riboprobes were synthesized from sequences from the 3′ untranslated region (UTR), and a dot blot procedure was used to quantify riboprobe yield. For *VanUV*, 309 bp of 3′UTR was used; for *VanB*, 492 bp of 3′UTR was used; and for *VanG*, 415 bp of 3′UTR was used.

The sections were then incubated in hybridization buffer (0.3 mM NaCl, 2.5 mM ethylene-tetraacetic acid, 20 mM Tris-Cl, pH 8.0, 50% formamide, 10% dextran sulfate, 200 μg/ml yeast tRNA, and 1× Denhart's medium; Sakamoto et al., 1996) in a humid chamber for 30 minutes at 60°C. The labeled probe was diluted in the hybridization buffer (1:100), corresponding to approximately 0.045 μg of probe per microliter of hybridization buffer. The sections were incubated in the diluted probe overnight at 55°C to 60°C in a humid chamber and then washed with 2×, 1×, and 0.1× standard saline citrate and 0.1% Tween, respectively, for 10 minutes each. The probes were located in the histologic sections by incubation with an anti-digoxigenin alkaline phosphatase–conjugated antibody (Boehringer Mannheim), diluted in 1× phosphate buffer plus Tween (1:1,000) for 2 hours. The probes were detected by a colorimetric reaction produced by nitro blue tetrazolium, 5-bromo-4-chloro-3-indolylphosphate, and 10% Tween in alkaline phosphatase developing solution.

Light microscopy

An Axioskop microscope (Zeiss, Thornwood, NY) equipped with differential interference contrast and brightfield and attached to an AxioCam digital camera (Zeiss) was used to collect images. Image data was recorded in the ZeissVision software on a personal computer in 2,060 × 2,600 pixel images through a 0.63 projection objective and a 5× dry, 10× dry, or 40× Neofluor oil lens. Selected images were digitally processed to enhance contrast or brightness in Adobe Photoshop 4.0.

RESULTS

Sequence data

The primer pair 80-RACE2 yielded a PCR product from cDNA with multiple bands when visualized on an agarose gel. From eight sequenced plasmids, three distinct opsin-encoding 3′RACE fragments were isolated. Each sequence

[2]The acute zone is the region of the eye that exhibits the greatest rate of spatial sampling. The fovea centralis of the human eye is an example of an acute zone.

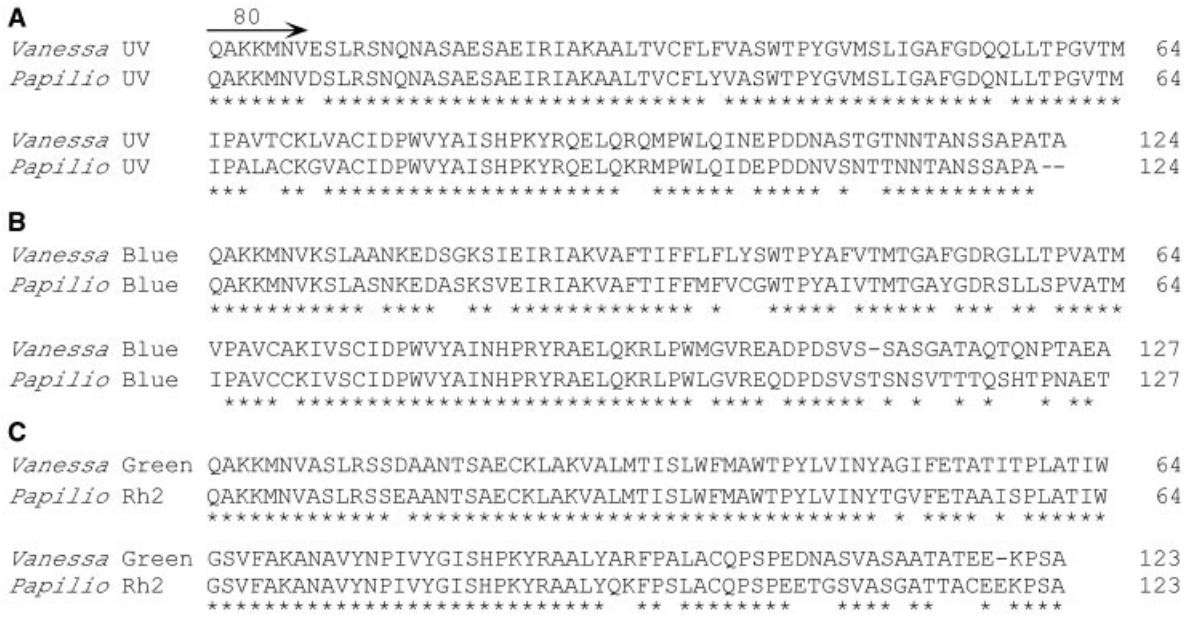

Fig. 2. Alignment of deduced amino acid sequences of cloned *Vanessa* 3′RACE products. **A:** *VanUV* opsin sequence. **B:** *VanB* opsin sequence. **C:** *VanG* opsin sequence. Asterisks indicate conserved amino acids relative to homologous opsin sequences from the butterfly, *Papilio glaucus*. The location of the primer 80 (EQAKKMN) is indicated by an arrow.

included part of the coding region and all of the 3′UTR. A BLAST search revealed homology of the three fragments to previously characterized butterfly UV-, blue-, and green-sensitive rhodopsins. The *VanUV* cDNA fragment (five clones) was collected in 684 bp, with the coding region consisting of 375 bp, or 125 predicted amino acids. The *VanB* cDNA fragment (one clone) was 873 bp in length, with the coding region consisting of 381 bp, or 127 predicted amino acids. The *VanG* cDNA fragment (two clones) was 820 bp, with the coding region consisting of 369 bp, or 123 predicted amino acids. No additional sequences were found when using two other sets of degenerate primers on cDNA and genomic DNA templates. The cDNA sequences were deposited in GenBank with the following accession numbers: AF414074 for *VanUV*, AF414075 for *VanB*, and AF385333 for *VanG*. An alignment of the deduced amino acid sequences is shown in Figure 2.

Phylogenetic analysis

All three models of nucleotide evolution (Kimura 2-parameter, HKY85, general time reversible) produced one tree (Fig. 3). Each of the three *Vanessa* opsin cDNA fragments was nested within other butterfly or moth opsin clades previously identified, respectively, as encoding UV-, blue-, or long wavelength-sensitive rhodopsins based on heterologous expression in a *Drosophila* transgenic system (Townson et al., 1998; Salcedo et al., 1999, and references therein).

Epi-microspectrophotometry of intact eyes

Calculation of the tapetal reflectance spectrum showed the spectrum to be constant for wavelengths shorter than 650 nm. The reason for constant reflectance over such a wide band is that the layer spacing varies by a factor of two, from one end of the tapetum to the other. Reflectance is relatively low at wavelengths longer than 700 nm because the largest spacing between tapetal platelets is too small to support constructive interference for reflected light at those wavelengths. The calculated tapetal reflectance spectrum and the experimental reflectance spectrum are shown in Figure 4A. Results of stripping the experimental reflectance spectrum of the contribution of the green-, blue-, and UV-sensitive rhodopsins are also shown in Figure 4A. When the contribution of a 395-nm substance is stripped from the residual, the modeled reflectance spectrum is a good fit of the tapetal reflectance spectrum (Fig. 4A).

The eye of *V. cardui* contains only three spectral types of visual pigment, P530, P470, and P360. Absorbance spectra for these pigments are shown in Figure 4B, the shape of which is based on the template of Stavenga et al. (1993). The solid dots in that figure represent an experimentally derived absorbance spectrum from Figure 1E of Bernard (1983b), which is a partial bleach created by repeated flashes of bright, long wavelength light. The high quality of fit supports the hypothesis there are no visual pigments that have λmax greater than 530 nm.

Retinal ultrastructure

Ommatidium. Figure 5A is a diagrammatic representation, drawn to scale, of an ommatidium measured from a limited sample of light and electron micrographs taken toward the center of the eye. In that region the ommatidia are about 510 μm from the surface of the cornea to the basement membrane that lies beneath the retina. They narrow from a diameter of about 30 μm at the corneal facet to about 25 μm at the basement membrane.

Dioptrics and pigment cells. The four Semper cells that enclose the crystalline cone are separated from the

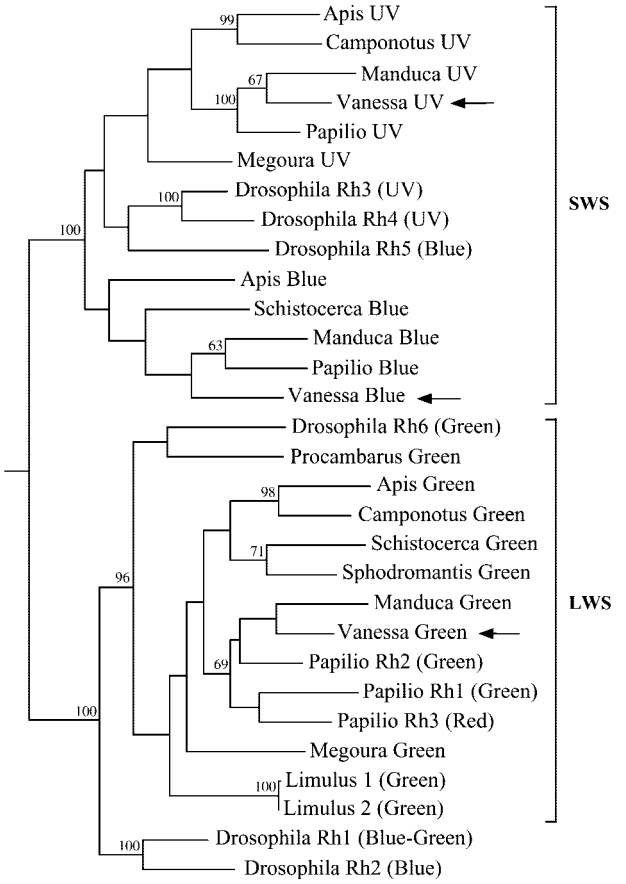

Fig. 3. Phylogeny of a diversity of invertebrate opsins. This tree is the result of a search using the neighbor-joining algorithm and HKY model of evolution. Numbers above the nodes indicate bootstrap values of 100 replicates. Only branches with bootstrap support greater than 50% are shown. Short and long wavelength-sensitive (SWS and LWS, respectively) opsin clades are indicated by brackets. Locations of *Vanessa* sequences are indicated by arrows.

cornea by an apparent extracellular space (designated the "corneal process" by Ribi, 1978) bounded by the two primary pigment cells. The cone terminates as a slender 1-μm process whose diameter matches that of the underlying rhabdom. The primary pigment cells are only sparsely pigmented. They narrowly encircle the Semper cells and then expand proximally to form an apron that caps the distal ends of the receptor cells. The distended ends of the primary pigment cells are packed with mitochondria and irregular empty vacuoles, an ultrastructure that suggests a unique function, perhaps in the photochemistry of rhodopsin chromophore (Pepe et al., 1982; Smith and Goldsmith, 1991). The secondary pigment cells (not included in Fig. 5) extend from the cornea to the basement membrane. Their expanded distal ends are heavily pigmented with 0.5-μm granules; proximally they narrow to slender processes before expanding again into a pigmented bulb at the basement membrane.

Retinula. The retinula is the assembly of photoreceptors of an ommatidium. It extends from the tip of the crystalline cone to the basement membrane, a span of about 420 μm at the center of the eye. Selected cross

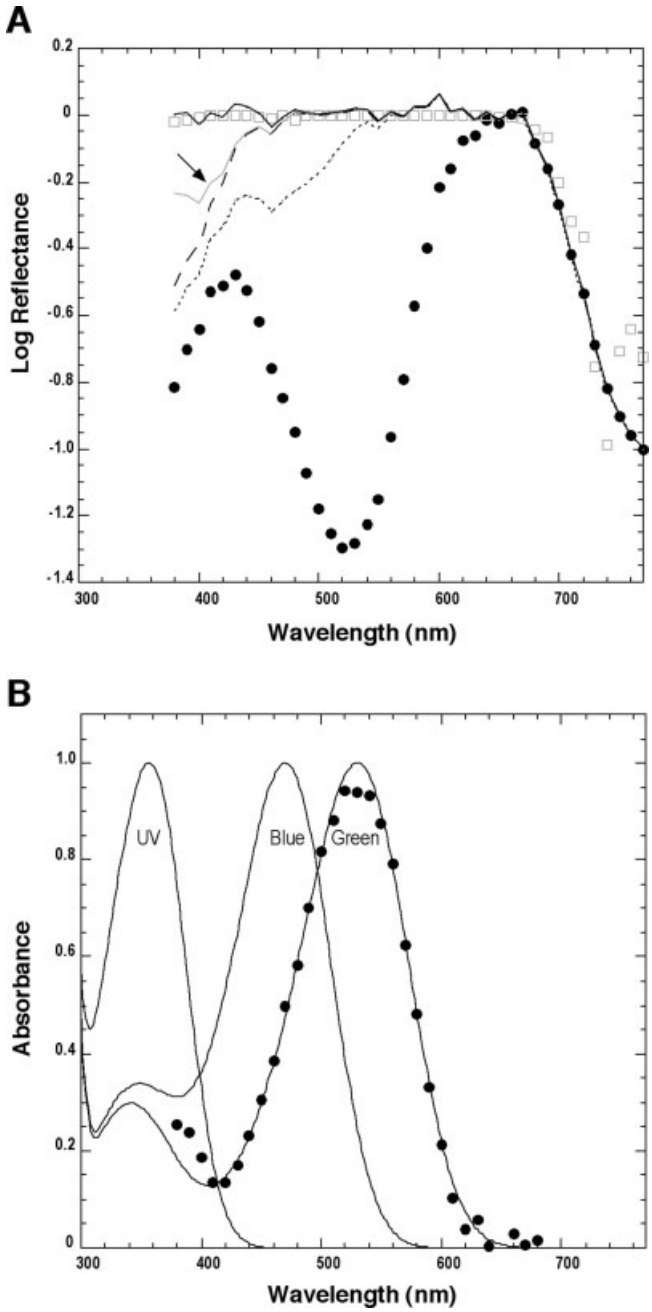

Fig. 4. **A:** Analysis of an experimental reflectance spectrum (dots) of *Vanessa cardui* eyeshine, based on a computational model of pigment content; dotted line, spectrum after having stripped density Dg = 0.62 of P530; dashed line, spectrum after having also stripped density Db = 0.12 of P470; solid gray line (arrow), spectrum after having also stripped density Duv = 0.15 of P360. The difference between the latter spectrum and the tapetal reflectance spectrum (open squares) is a residual well fit by density Dp = 0.11 of a putative retinoid-binding protein (black line). **B:** Normalized absorbance spectra for the three spectral types of rhodopsin for *V. cardui*, peaking in the UV (P360), blue (P470), and green (P530) spectra. The solid curves are idealized spectra based on the A_1 and SSH template (Stavenga et al., 1993). The solid dots represent an experimentally derived normalized absorption spectrum for P530 from a completely intact *V. cardui*, based on Figure 1E of Bernard (1983a).

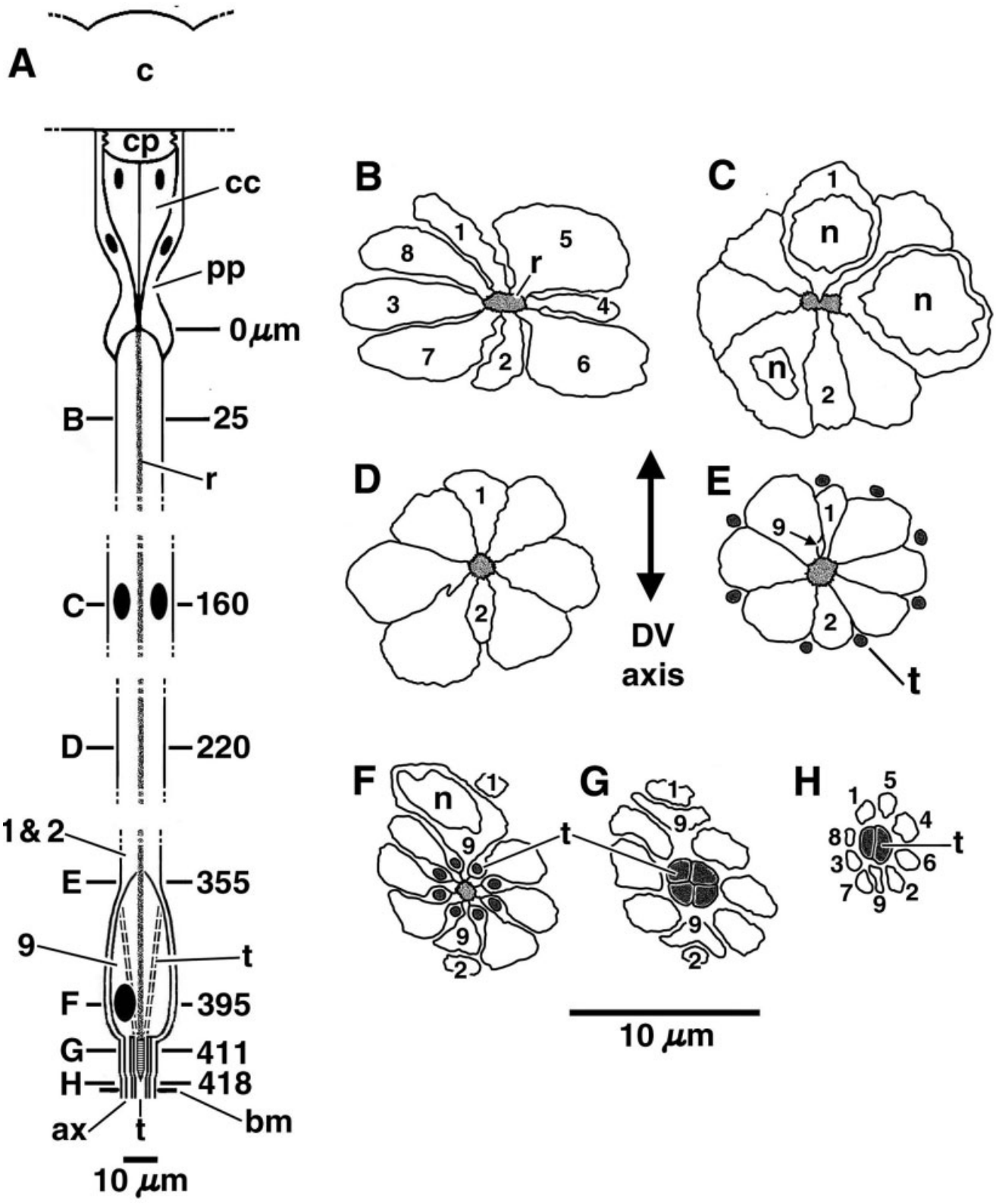

Fig. 5. **A:** Schematic of a longitudinally drawn ommatidium, with fused rhabdom and R1 and R2 photoreceptor cell bodies shown. Black ovals indicate nuclei of crystalline cones; primary pigment cells; and R1, R2, and R9 photoreceptor cells. **B–H:** Tracings from electron micrographs of individual ommatidia at different levels in the retina. Locations of sections from the distal tip of photoreceptor cell are as follows: 25 μm (B), 160 μm (C), 220 μm (D), 355 μm (E), 395 μm (F), 411 μm (G), and 418 μm (H). Basement membrane (bm), 420 μm. Photoreceptor cells are numbered 1 through 9. Light gray areas indicate fused rhabdom. Dark gray areas indicate locations of tracheoles (t). c, cornea; cc, crystalline cone; n, nucleus; pp, primary pigment cell.

sections of the retinula traced from electron micrographs are shown in Figure 5B–H. The diameter of the retinula is nearly constant, about 12 μm, except as it expands to about 16 μm at the nuclear level (Fig. 5C). As is characteristic of the lepidopteran retinula, it consists of nine photoreceptor cells (designated R1 through R9, according to the convention of Ribi, 1987): eight elongate cells (R1 to R8) extending from the cone to their synaptic termini in the visual centers of the brain and one smaller cell (R9; Fig. 5E–G) extending from about 40 μm above the basement membrane to its synaptic terminus in the brain. Screening pigment is concentrated at the distal ends of R1 through R8. Larger, irregular globules that stain densely with osmium are found more proximally. These appear dark yellow in aldehyde-fixed retinas; they may be carotenoid-containing oil droplets. R9 appears more darkly stained with osmium than the other receptors owing to the density of mitochondria, endomembrane, and granular cytosolic material.

Receptor cells R1 and 2 and the bilobed cell R9 are oriented along the dorsal-to-ventral axis of the eye; R3 and R4 are oriented in anterior-to-posterior axis; R5 through R8 are oriented obliquely. In Figure 5B–H, only the axes of the eye can be determined. Thus R1, the dorsal cell, could not be distinguished from its ventral twin, R2, and we could not tell whether the nucleus and axon of R9 were positioned, respectively, on the dorsal and ventral sides of retinula as shown or in the reverse orientation.

Rhabdom. The diameter of the fused rhabdom (Fig. 6A) remains close to 2 μm along its entire length. Its constituent microvilli contributed by the nine receptors are organized in longitudinal layers, as described by Maida (1977), Gordon (1977), and Kolb (1985). We did not characterize the relative contributions of the different receptors to the rhabdom along its length, except that the rhabdomeres of R1 and R2 are larger distal to the nuclear region, that is, in the distal 160 μm of the retinula. There is a specialized region of the retina consisting of two rows of ommatidia at the dorsal rim of the eye. These have rectangular rhabdoms whose rhabdomeres contribute orthogonally oriented microvilli (Fig. 6B), characteristic of the dorsal rim polarized light detectors described in many insects (Labhart and Meyer, 1999), including the butterfly *Aglais* (Kolb, 1986).

Tracheoles and tapetum. One tracheole cell, surrounded by the nine photoreceptor axons, with its nucleus below the basement membrane (Fig. 6E), subtends each ommatidium. The tracheole trunk penetrates through the basement membrane (Fig. 6C), dividing into two branches (Fig. 5H), then four branches (Fig. 5G), and then eight branches (Fig. 5F). In the region of the ninth cell, the eight tracheole branches lie between the receptor cells (Fig. 5F). More distally they shift to the periphery of the retinula (Fig. 5E) and then extend irregularly through the distal retina (not shown in Fig. 5B–D). In the quadripartite region of the tracheole underlying the ninth cell, the tracheal taenidia are precisely spaced to provide a tapetal interference reflector that reflects light of selective wavelengths back into the rhabdom (Miller and Bernard, 1968; Miller, 1979).

A dorsal-to-ventral patterning difference in the distribution of *VanB* mRNA

In situ hybridizations performed in parallel with sense and antisense riboprobes showed that the sense strand riboprobes did not hybridize to paraformaldehyde-fixed cryostat-sectioned retinas (data not shown), whereas antisense strand riboprobes did (Figs. 7–10). *VanUV* (Fig. 7A) and *VanB* (Fig. 7B) mRNAs were distributed throughout the retina in longitudinal sections and to different degrees along the dorsal-to-ventral axis. The *VanUV* mRNA was distributed dorsally and ventrally in the retina, with a somewhat lighter distribution in the central portion of the ventral retina and a heavier distribution at the edge of the ventral retina and in the dorsal portion of the retina (Fig. 7A). The *VanB* mRNA had sparse distribution in the dorsal retina and heavy distribution in the ventral retina (Fig. 7B). Alternately stained (*VanUV* in Fig. 7A and *VanB* in Fig. 7B), adjacent retinal longitudinal sections showed that, where the *VanUV* mRNA expression dropped off in the retina, the *VanB* mRNA expression picked up. This pattern was observed in all six individuals sampled. These patterns of *VanUV* and *VanB* mRNA expression in whole-retina longitudinal sections suggested that the *VanUV* and *VanB* mRNAs are expressed in a complementary manner.

VanUV and *VanB* opsin mRNAs are expressed in nonoverlapping R1 and R2 photoreceptor cells

Longitudinal sections through the retina hybridized to the *VanUV* riboprobe indicated the presence of three kinds of ommatidia: those in which both members of a pair of photoreceptor cells express the transcript, those in which one but not the other express it, and those in which neither cell express it (Fig. 7C). Cross sections through the posterior edge of the left eye stained with the same *VanUV* probe identified these cells as R1 and R2 cells, characterized by their dorsal-to-ventral axis of orientation (Fig. 8).

VanUV (Fig. 9A) and *VanB* (Fig. 9B) riboprobes hybridized to adjacent tangential sections revealed complementary *VanUV* and *VanB* mRNA expression in R1 and R2 photoreceptor cell bodies. The distribution of *VanUV* and *VanB* mRNAs among the R1 and R2 cells indicated three classes of ommatidia. No staining was observed in the photoreceptor cell bodies R3 through R8 with the *VanUV* or the *VanB* riboprobes.

VanUV *mRNA distribution.* In the majority of the retina, the *VanUV* mRNA was expressed in nearly all R1 and R2 photoreceptor cell bodies. Specifically, most ommatidia contained R1 and R2 cells that expressed only *VanUV* mRNA. More rarely, some ommatidia contained one R1 or R2 cell that expressed the *VanUV* mRNA (double arrowheads in Fig. 9A); even more rarely, some ommatidia contained R1 and R2 cells that expressed no *VanUV* mRNA (arrow in Fig. 9A).

VanB *mRNA distribution.* Everywhere in the retina except in a portion of the ventral retina (Fig. 7B), the *VanB* mRNA was sparsely distributed. Most ommatidia entirely lacked *VanB* mRNA expression in the R1 and R2 cells. Occasionally, some ommatidia were found that contained one R1 or R2 cell that expressed the *VanB* mRNA (arrowheads, Fig. 9B); even more rarely, some ommatidia were found that expressed the *VanB* mRNA in R1 and R2 cells simultaneously (arrows, Fig. 9B).

A count of 156 ommatidia shown in Figure 9A included 106 (67.9%) ommatidia in which R1 and R2 cells expressed the *VanUV* mRNA, 46 (29.5%) in which only one of the two cells expressed the *VanUV* mRNA, and four (2.6%) in

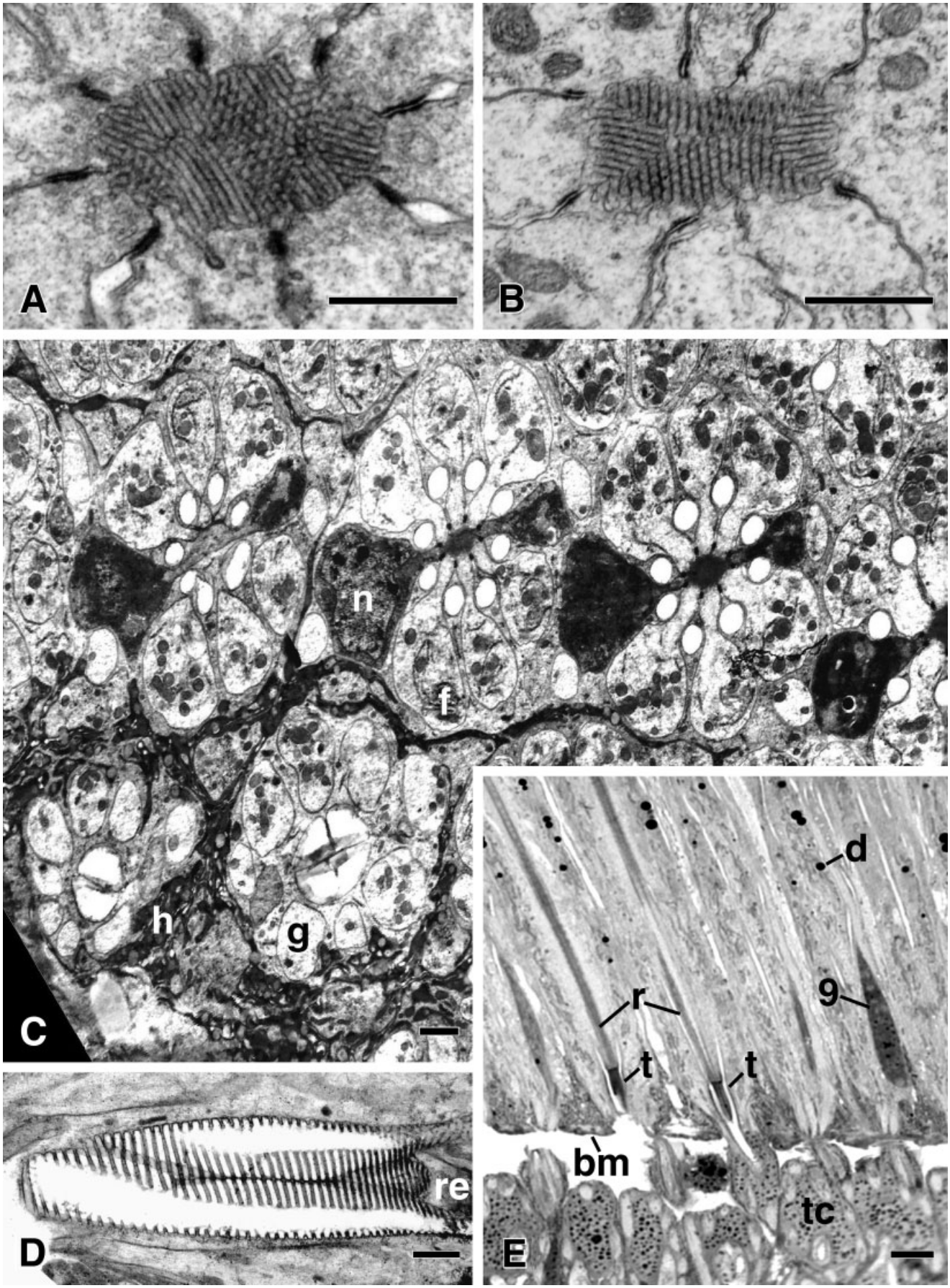

Figure 6

which neither cell expressed it. As a control, the same ommatidia were counted for *VanB* expression (Fig. 9B), and four (2.6%) ommatidia were identified in which both cells contained *VanB* mRNA, 46 (29.5%) were identified with one or the other cell expressing *VanB* mRNA, and the other 106 (67.9%) did not express the mRNA in either cell. No ommatidium in this portion of the retina was identified in which neither the *VanUV* nor the *VanB* transcripts could be localized to the R1 and R2 photoreceptor cells.

VanG mRNA is expressed in R3 through R8 cell bodies in the main retina

The R3 through R8 photoreceptor cells have unique properties compared with the R1 and R2 cells. Only the *VanG* mRNA was expressed in these six cells in all ommatidia in the retina. This was observed in longitudinal sections hybridized to the *VanG* riboprobe (data not shown), in dissociated ommatidia (Fig 10A), and in tangential sections of the retina (Fig. 10B). The *VanG* mRNA expression levels appeared to be more or less uniform in all R3 through R8 photoreceptor cells throughout the retina. In addition, the cross-sectional areas of the R3 through R8 cells were somewhat larger than those of the R1 and R2 cells as estimated from the positive *VanG* mRNA staining of the R3 through R8 cells in tangential sections (Fig. 10B) relative to the absence of staining in the R1 and R2 cells in the same section. Similarly, the R1 and R2 cell bodies appeared much narrower in dissociated ommatidia stained for the presence of the *VanB* mRNA (Fig. 10D,E) than did the R3 through R8 cell bodies stained for the presence of *VanG* mRNA (Fig. 10A). These observations complemented findings from ultrastructure (Fig. 5B,D,E) that the R1 and R2 cells are narrower than the R3 through R8 cells.

VanG mRNA is localized to the R9 photoreceptor cell body

In addition to *VanG* mRNA expression in the R3 through R8 cells, *VanG* mRNA expression was observed in the small R9 photoreceptor cell that subtended the other eight just above the basement membrane (arrows, Fig. 10A,C). The R9 cell had a bilobed structure (Figs. 5F,G, 6C,E) that facilitated the identification of this cell in dissociated ommatidia (Fig. 10A,C). All ommatidia in which we were able to positively identify the R9 cell expressed this *VanG* transcript.

Three kinds of ommatidia are present in the retina with respect to *VanUV*, *VanB*, and *VanG* mRNA expression

The in situ results indicated that there are eight elongate (R1 to R8) and one small bilobed (R9) photoreceptor cells in each ommatidium. Six of these elongate photoreceptor cells (R3 through R8) were approximately equal in size and shape to one another and collectively larger than the two other elongate photoreceptor cells, R1 and R2. In terms of the distribution of opsin mRNAs, one pair of cells (R1 and R2) expressed *VanB* or *VanUV* mRNAs in a complementary manner, and the other seven (R3 through R9) expressed *VanG* opsin mRNA. Each ommatidium expressed the opsin mRNAs differently from neighboring ommatidia and in combination produced at least three different classes of ommatidia. (Because we did not investigate the expression pattern of opsins in the dorsal rim, we cannot exclude the possibility that other classes of ommatidia are present in the adult *Vanessa* retina.) One class expressed the *VanUV* and *VanG* opsin mRNAs; another expressed the *VanB* and *VanG* opsin mRNAs; and the third expressed all three (*VanUV*, *VanB*, and *VanG*). Most ommatidia expressing all three opsin mRNAs appeared to be localized to a portion of the ventral retina (Fig. 7A,B), whereas most ommatidia expressing only *VanUV* and *VanG* were in the dorsal retina. Scattered throughout the dorsal retina were a few ommatidia with *VanB* mRNA expression (Fig. 7B).

DISCUSSION

Epi-microspectrophotometry of intact eyes

Results from analysis of the experimental reflectance spectrum and the computational model suggested that, in addition to UV-, blue-, and green-absorbing rhodopsins, the rhabdoms contain a small amount of a substance having an absorption spectrum similar to a visual pigment of 395-nm λmax, but which makes no contribution to the electroretinogram (ERG) spectral sensitivities in the experiments of Chen (1987) under different states of chromatic adaptation. What could that substance be? Based on our knowledge from several, quite different experimental techniques, it is certainly not a visual pigment (11-*cis*-chromophore attached to a membrane-bound opsin). A better hypothesis is that the substance with a peak absorbance at 395 nm is involved in the cycle of visual pigment renewal. As described by Bernard (1983b), we know that the photoproduct M490 decays very rapidly from the rhabdom at elevated temperature, and that visual pigment P530 recovers rapidly in the dark but at a slower rate and with different kinetics than those for decay of M490. Most likely, the all-*trans* retinaldehyde chromophores of M490 are hydrolyzed from their opsin-binding site. Then, because retinaldehyde is so very reactive, the liberated chromophores bind to soluble proteins. The rapid dark regeneration of P530 could involve a retinoid-binding protein that transports re-isomerized 11-*cis*-chromophore. Precedence for two such retinoid-binding proteins in insect eyes (bees) was published by Pepe et al. (1982).

Fig. 6. Micrographs of *Vanessa cardui* retina. **A:** Electron micrograph of rhabdom from a distal region of retinula (between levels B and C in Fig. 5) near the center of the eye. **B:** Rhabdom from a distal region of dorsal rim retinula. The sections shown in A and B provide slightly oblique profiles of circular (A) and square (B) rhabdoms. Receptor cells R1 and R2 are oriented vertically. **C:** Electron micrograph from a region near the basement membrane showing cross-sectioned retinulae. The dense cytoplasm of bilobed receptor cell R9 is darkly stained. Retinulae at levels F, G, and H in Figure 5 are labeled f, g, and h. Receptor cell axons surround the bipartite tracheole in retinula h and the quadripartite tracheole in g. The nucleus (n) of cell R9 is seen in retinula f. The six ultimate tracheole branches lying between the receptor cells are seen in the other retinulae. **D:** Electron micrograph of a longitudinal section of quadripartite tracheole underlying the retinula (re) whose taenidial reflector functions as a tapetum. Measurements from this micrograph were used to calculate the tapetal reflectance spectrum in Figure 4A. **E:** Light micrograph of a longitudinal section of proximal retina bounded by the basement membrane (bm). Tracheole interference reflectors (t) can be seen underlying their rhabdoms (r). The tracheole cell bodies (tc), recognized from their speckled nuclei, lie beneath the basement membrane. d, receptor cell oil droplet; 9, receptor cell R9. Scale bars = 1 μm in A–D, 10 μm in E.

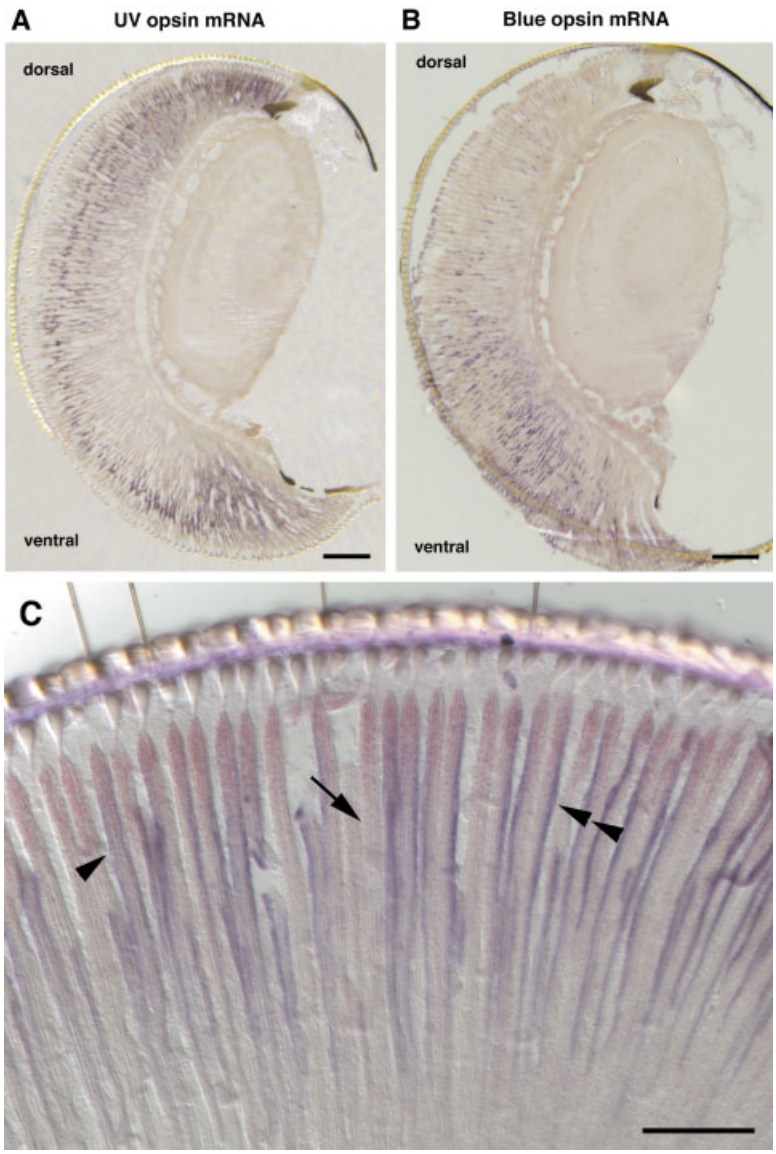

Fig. 7. Localization of *VanUV* and *VanB* mRNAs by hybridization of digoxigenin-labeled antisense riboprobes to adjacent 20-μm longitudinal sections of the *Vanessa* retina. **A:** *VanUV* mRNA expression is distributed across the majority of the retina, although less heavily so in a ventral portion of the eye. **B:** *VanB* mRNA expression is restricted mostly to the ventral retina, with very little expression in the dorsal retina. **C:** Longitudinal section through the retina show three classes of ommatidia with respect to *VanUV* mRNA expression in a pair of opposing photoreceptor cells: no expression (arrow), expression in one member of the pair (double arrowhead), and expression in both cells (single arrowhead). Scale bars = 200 μm in A and B, 100 μm in C.

Ultrastructure and spectral sensitivities of photoreceptor cells in the nymphalid retina

The structure of the *V. cardui* ommatidium is similar to that described for other butterflies (*Pieris*: Kolb, 1977; Maida, 1977; Qiu et al., 2002; *Papilio*: Ribi, 1987) especially that of other nymphalids (*Agraulis*: Gordon, 1977; *Aglais*: Kolb, 1985). Previous attempts at characterizing the spectral sensitivities of individual classes of photoreceptor cells in the retina of nymphalid butterflies that are closely related to *Vanessa* (Nymphalini) have generally found UV-, blue-, and green-sensitive classes of photoreceptor. Kolb (1985), for instance, found the nymphalid *Aglais urticae* (Nymphalini) to have these three classes of receptor. By using adaptation experiments in which she traced the migration of photoreceptor cell pupillary pigments during light treatment, Kolb assigned UV sensitivity to the R1 and R2 photoreceptor cells and green sensitivity (λmax $\sim$ 520 nm) to the R5 through R8 photoreceptor cells. The results of our in situ hybridization experiments are in good agreement with her conclusions about the assignment of UV and green sensitivities to these cell types. She was less certain about the distribution of the blue-sensitive photoreceptor cell classes. Based on an analysis of the relative sensitivities of blue-

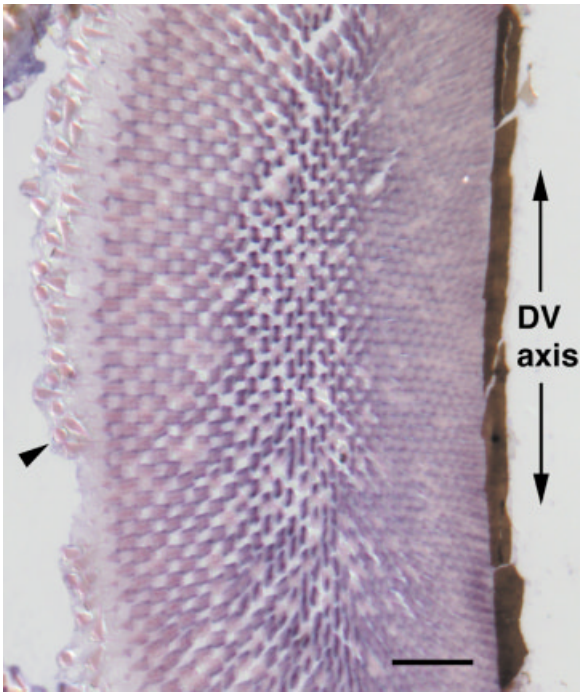

Fig. 8. Cross section through the posterior margin of the left eye showing the orientation of the *VanUV* mRNA-expressing photoreceptor cells relative to the vertical axis of the eye. The dorsal–ventral (DV) orientation of these cells indicate that they are identical to the R1 and R2 photoreceptor cells characterized ultrastructurally (Fig. 5). Most R1 and R2 cells in this region express the *VanUV* transcript. Arrowhead indicates crystalline cones. Scale bar = 50 μm.

absorbing rhodopsins characterized in *A. urticae* by Steiner et al. (1987), Kolb concluded that it was questionable whether all ommatidia contained blue-sensitive photoreceptor cells. In our study of the *Vanessa* retina, we found the distribution of blue-sensitive opsin-encoding mRNAs to be much less than that of the UV ones and restricted mostly to the ventral portion of the retina. Although *Aglais* and *Vanessa* are different species that might harbor other differences in their pattern of opsin mRNA expression, this finding is in agreement with the behavioral work of Aleibak (1981) on *Aglais* showing a significant preference for blue (λmax = 467 nm) in spontaneous-choice feeding experiments. The ventral portion of the retina, closest to the surface of flowers in this sort of experiment, might be particularly suited for visual input required for this kind of behavior. That is the portion of the retina where we found the highest concentration of blue opsin mRNA.

More recent work on the nymphalid butterfly *Polygonia aureum* (Nymphalini) has involved the use of polarized light to identify the spectral properties of individual photoreceptor cell classes. Kinoshita et al. (1997) found that the R1 and R2 cells have microvilli that are parallel to the vertical axis of the eye and are UV or blue sensitive; the R3 and R4 cells have microvilli that are aligned horizontally and are green sensitive, and the R5 through R8 cells have diagonally oriented microvilli that are also green sensitive. Although we did not determine the orientation of the microvilli throughout the entire length of a retinula, these results from related species are consistent with the distribution of UV-, blue-, and green-sensitive opsin-encoding mRNAs in *V. cardui*.

Distribution of opsin expression among *Vanessa* photoreceptor cells in comparison to *Papilio*

In addition to the λmax values of the rhodopsins, their densities and the ultrastructure of the retina, we described the expression patterns of *VanUV*, *VanB*, and *VanG* opsin mRNAs in the retina of the adult butterfly, *V. cardui*. These methods showed that photoreceptor-specific localizations of the *VanUV* and *VanB* opsin mRNAs in the R1 and R2 photoreceptor cells are similar (but not identical) to those described for the homologous opsin mRNAs in the papilionid butterfly *Papilio xuthus* (Kitamoto et al., 2000). As in *P. xuthus*, three types of ommatidia were found in the retina with respect to the expression of the UV- and blue-sensitive rhodopsin mRNAs: those that express the UV-sensitive rhodopsin mRNA in R1 and R2 cells, those that express only the blue-sensitive rhodopsin mRNA in these cells, and those that express the UV-sensitive rhodopsin transcript in one cell and the blue-sensitive rhodopsin transcript in the other. The retinas of *V. cardui* and *P. xuthus* differ with respect to the distribution of the UV- and blue-sensitive rhodopsin mRNAs in one important respect. A dorsal-to-ventral patterning difference was observed in the distribution of *VanB* mRNA in the retina of *V. cardui* that differs from the distribution of the blue-sensitive rhodopsin mRNA reported for *P. xuthus*. In *V. cardui*, *VanB* mRNA is nearly absent from the dorsal portion of the retina and heavily distributed in a portion of the ventral retina; in *P. xuthus*, the homologous blue-sensitive rhodopsin-encoding mRNA is most heavily expressed in the dorsal retina (Kitamoto et al., 2000). This difference extends to the distribution of homologous UV-sensitive rhodopsin-encoding mRNAs in the retinas of both species of butterfly. The ventral retina of *P. xuthus* has a larger proportion of UV-sensitive rhodopsin mRNA-expressing R1 and R2 photoreceptors than does the dorsal retina (Kitamoto et al., 2000), whereas the ventral retina of *V. cardui* appears to contain mostly *VanUV*-expressing R1 and R2 cells.

We also found that, unlike *P. xuthus*, *V. cardui* has one green-sensitive rhodopsin-encoding mRNA (*VanG*) that can be localized to R3 through R9 photoreceptor cells in the retina. *Papilio xuthus* has three duplicated LWS opsin genes whose mRNAs have been shown to be differentially expressed in the retina (Kitamoto et al., 1998). By using riboprobes synthesized from the 3′UTRs, Kitamoto et al. (2000) showed that each of the duplicated LWS opsin mRNAs has photoreceptor cell-specific patterns of expression. For instance, *PxRh1* is co-expressed with *PxRh2* in the R3 and R4 photoreceptor cells in the ventral retina (Kitamoto et al., 1998). In the dorsal retina, the R3 and R4 cells express only *PxRh2*; *PxRh1* expression is absent. Hence, the *P. xuthus* retina has a dorsal-to-ventral patterning difference in the expression of an LWS opsin-encoding mRNA that is not observed in *Vanessa*, which appears to lack these duplicated opsins. In addition, the R5 through R8 photoreceptor cells of *P. xuthus* were shown to have a complex pattern of opsin expression with regard to the distribution of *PxRh2* and *PxRh3* transcripts. Although most R5 through R8 photoreceptor cells

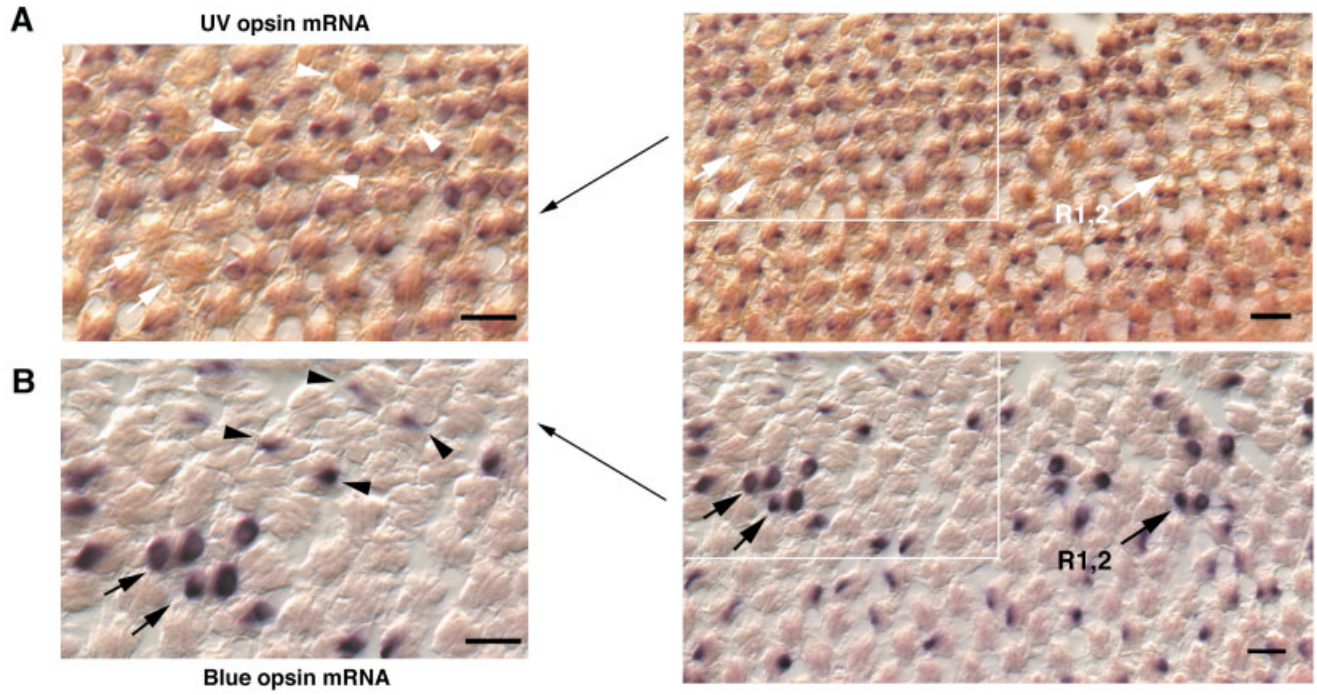

Fig. 9. Localization of *VanUV* and *VanB* mRNAs by hybridization of antisense riboprobes to adjacent 16-μm cross sections of the *Vanessa* retina showing complementary expression of *VanUV* and *VanB* mRNAs in the R1 and R2 cells. **A:** *VanUV* mRNA expression. Arrows indicate ommatidia where *VanUV* mRNA expression is absent in R1 and R2 cells. Arrowheads indicate ommatidia where *VanUV* mRNA expression is absent in the R1 or R2 cell but in not both. **B:** *VanB* opsin mRNA expression. Arrows indicate ommatidia where R1 and R2 cells express the blue opsin transcript. Arrowheads indicate ommatidia where *VanB* mRNA transcripts are expressed in the R1 or R2 cells but not in both. Aligned arrows and arrowheads point to the same ommatidia in adjacent sections. Scale bars = 20 μm in A and B.

in an individual ommatidium express *PxRh2* or *PxRh3*, a small number of ommatidia in the *P. xuthus* retina were found to co-express both transcripts. These results have been confirmed by examining the homologous opsin mRNA expression patterns in the butterfly *Papilio glaucus* (Briscoe and Nagy, unpublished). Kitamoto et al. (2000) also found that *PxRh1* and *PxRh2* are expressed in the R9 photoreceptor cell body in *P. xuthus*. In *Vanessa* we found only the green-sensitive rhodopsin mRNA in the R9 photoreceptor cells.

Our novel gene expression data from *V. cardui* (Nymphalidae), in combination with a robust opsin phylogeny and comparative gene expression data from *P. xuthus* (Papilionidae) (Kitamoto et al., 1998, 2000), allows a consideration of how the retinal expression patterns of opsins may have evolved in butterflies. Phylogenetically, the *P. xuthus* opsin *PxRh2* is most closely related to the clade of nymphalid opsins that contains the *Vanessa VanG* opsin and is ancestral to *PxRh1* and *PxRh3* (Fig. 1). Of the three transcripts, *PxRh2* has the broadest distribution: in the R3 through R9 photoreceptor cells, as does the *Vanessa VanG* mRNA. In contrast, both duplicated *PxRh1* and *PxRh3* opsin genes have expression patterns that lie in subsets of these cells, in the case of *PxRh1* in R3, R4, and R9 cells and in the case of *PxRh3* in R5 through R8 cells. Elsewhere (Briscoe, 2001) we argued that the *PxRh1* pattern of gene expression is a good example of what Force et al. (1999) described as a "partitioning of ancestral function rather than the evolution of new functions," because the spectral sensitivities of the photoreceptor cells in which *PxRh1* and *PxRh2* are expressed are known to be maximally sensitive to green light (Bandai et al., 1992). In contrast, *PxRh3* may be an example of a duplicated gene that has acquired a new function because it is expressed in a subset of cells that are known to be red sensitive (Bandai et al., 1992, Arikawa and Uchiyama, 1996). As we documented through photochemical experiments, a red-sensitive rhodopsin was not observed in the *Vanessa* retina. The lack of red-absorbing rhodopsins, the phylogenetic placement of the *Vanessa* green opsin in a clade that appears to be most closely-related to the most ancestral of the three *Papilio* LWS retinal opsins, *PxRh2*, and the presence of only one green opsin transcript in the *Vanessa* retina suggested that *Vanessa* has a visual system that is more similar in patterning to the ancestral lepidopteran eye than to *Papilio*. Indeed, the handful of studies of moth retinas suggested that moths have three common rhodopsins: UV, blue, and green absorbing (Bennett and Brown, 1985; Briscoe and Chittka, 2001). A physiological study also suggested that the ventral distribution of the blue-sensitive rhodopsin transcript we described in *Vanessa* may be found in moths. Bennett et al. (1997) found the ventral retina of the moth *Manduca sexta* to have the greatest blue sensitivity, and a distribution of rhodopsins similar to that found in *Vanessa* was shown by immunocytochemistry (R.H. White, unpublished observations). Further studies are

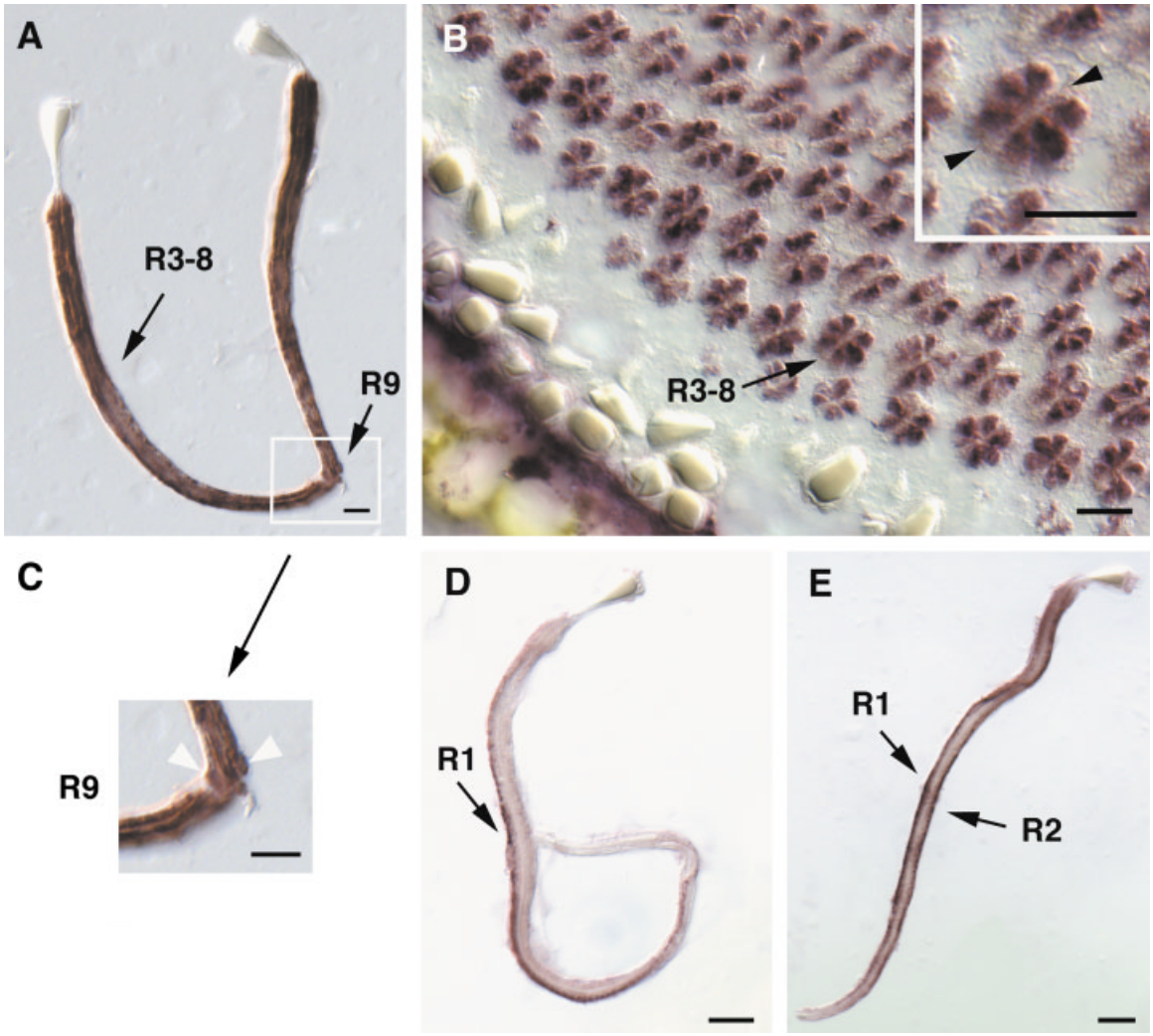

Fig. 10. In situ hybridizations of green and blue opsin riboprobes to dissociated ommatidia and a cross-section of the *Vanessa* retina. **A:** Two dissociated ommatidia joined at the basement membrane with attached cornea and crystalline cones (unstained) and R1 through R9 photoreceptor cells stained with the *VanG* riboprobe. Arrows indicate ommatidium magnified in inset. **B:** Cross section of retina showing the localization of the *VanG* mRNA transcript. Arrow indicates stained R3 through R8 photoreceptor cells. **Inset:** R3 through R8 photoreceptor cells are stained; R1 and R2 are unstained (arrowheads). **C:** Magnified view of R9 cell showing *VanG* mRNA transcript. Arrowheads indicate individual lobes of the bilobed R9 cell. **D:** Dissociated ommatidium showing distribution of *VanB* mRNA in one R1 or R2 cell (arrow). **E:** Dissociated ommatidium showing expression of the *VanB* mRNA in R1 and R2 photoreceptor cells. Scale bars = 20 μm in A–E and inset.

needed to verify the extent to which this pattern is found across Lepidoptera.

ACKNOWLEDGMENTS

We thank Dr. Steven Britt (S.B.) for the use of his laboratory while the studies were being completed; Dr. Joan Hooper for her help and advice regarding brightfield microscopy and digital photography; and Erin Smith and Meridee Phistry for technical assistance. We also thank Gail Burd, Elizabeth Jockusch, Dave Lambert, Candice Nulsen, and James Cooley for their technical advice. Eve Bagg, Denise Berkholz, and Ruth Fulton provided comments on the figures. Two anonymous reviewers provided especially excellent editorial remarks.

LITERATURE CITED

Alaibak A. 1981. Verhaltensversuche zur Farbpräferenz von *Aglais urticae* L. (Lepidoptera) [Diplomarbeit]. Munich: Ludwig-Maximilian-Universität München.

Arikawa K, Stavenga D. 1997. Random array of colour filters in the eyes of butterflies. J Exp Biol 200:2501–2506.

Arikawa K, Uchiyama H. 1996. Red receptors dominate the proximal tier of the retina in the butterfly *Papilio xuthus*. J Comp Physiol A 178:55–61.

Arikawa K, Mizuno S, Scholten DGW, Kinoshita M, Seki T, Kitamoto J, Stavenga DG. 1999. An ultraviolet absorbing pigment causes a narrow-band violet receptor and a single-peaked green receptor in the eye of the butterfly *Papilio*. Vis Res 39:1–8.

Bandai K, Arikawa K, Eguchi E. 1992. Localization of spectral receptors in the ommatidium of butterfly compound eye determined by polarization sensitivity. J Comp Physiol A 171:289–297.

Bennett RR, Brown PK. 1985. Properties of the visual pigments of the moth *Manduca sexta* and the effects of two detergents, digitonin and chaps. Vis Res 25:1771–1781.

Bennett RR, White RH, Meadows J. 1997. Regional specialization in the eye of the sphingid moth *Manduca sexta*: Blue sensitivity of the ventral retina. Vis Neurosci 14:523–526.

Bernard GD. 1975. Physiological optics of the fused rhabdom. In: Snyder AW, Menzel R, editors. Photoreceptor optics. New York: Springer-Verlag. p 78–97.

Bernard GD. 1979. Red-absorbing visual pigment of butterflies. Science 203:1125–1127.

Bernard GD. 1982. Noninvasive optical techniques for probing insect photoreceptors. In: Packer L, editor. Methods in enzymology. Volume 81. New York: Academic Press. p 752–759.

Bernard GD. 1983a. Bleaching of rhabdoms in eyes of intact butterflies. Science 219:69–71.

Bernard GD. 1983b. Dark-processes following photoconversion of butterfly rhodopsins. Biophys Struct Mech 9:277–286.

Bernard GD, Remington CL. 1991. Color vision in *Lycaena* butterflies: spectral tuning of receptor arrays in relation to behavioral ecology. Proc Natl Acad Sci USA 88:2783–2787.

Brekhovskikh LM. 1960. Waves in layered media. New York: Academic Press. p 21–33.

Briscoe AD. 1998. Molecular diversity of visual pigments in the butterfly *Papilio glaucus*. Naturwissenschaften 85:33–35.

Briscoe AD. 1999. Intron splice sites of *Papilio glaucus PglRh3* corroborate insect opsin phylogeny. Gene 230:101–109.

Briscoe AD. 2000. Six opsins from the butterfly *Papilio glaucus*: molecular phylogenetic evidence for paralogous origins of red-sensitive visual pigments in insects. J Mol Evol 51:110–121.

Briscoe AD. 2001. Functional diversification of lepidopteran opsins following gene duplication. Mol Biol Evol 18:2270–2279.

Briscoe AD, Chittka L. 2001. The evolution of color vision in insects. Annu Rev Entomol 46:471–510.

Chase MR, Bennett RR, White RH. 1997. Three opsin-encoding cDNAs from the compound eye of *Manduca sexta*. J Exp Biol 200:2469–2478.

Chen DM. 1987. Ultraviolet sensitivity in compound eye of the butterfly *Vanessa cardui*. Acta Entomol Sin 30:353–358.

Force A, Lynch M, Pickett F, Amores A, Yan YL, Postlethwait J. 1999. Preservation of duplicate genes by complementary, degenerative mutations. Genetics 151:1531–1545.

Gordon WC. 1977. Microvillar orientation in the retina of the nymphalid butterfly. Z Naturforsch 32c:662–664.

Hsu R, Briscoe AD, Chang BSW, Pierce NE. 2001. Molecular evolution of a long wavelength-sensitive opsin in mimetic *Heliconius* butterflies (Lepidoptera: Nymphalidae). Biol J Linn Soc 72:435–449.

Ilse D. 1965. Versuche zur Orientierung von Tagfaltern. Verh Dtsch Zool Ges, Jena 59:306–319.

Jiggins CD, Naisbit RE, Coe RL, Mallet J. 2001. Reproductive isolation caused by colour pattern mimicry. Nature 411:302–305.

Kelber A. 1999. Ovipositing butterflies use a red receptor to see green. J Exp Biol 202:2619–2630.

Kinoshita M, Sato M, Arikawa K. 1997. Spectral receptors of nymphalid butterflies. Naturwissenschaften 84:199–201.

Kitamoto J, Sakamoto K, Ozaki K, Mishina Y, Arikawa K. 1998. Two visual pigments in a single photoreceptor cell: identification and histological localization of three mRNAs encoding visual pigment opsins in the retina of the butterfly *Papilio xuthus*. J Exp Biol 201:1255–1261.

Kitamoto J, Ozaki K, Arikawa K. 2000. Ultraviolet and violet receptors express identical mRNA encoding an ultraviolet-absorbing opsin: identification and histological localization of two mRNAs encoding short-wavelength–absorbing opsins in the retina of the butterfly *Papilio xuthus*. J Exp Biol 203:2887–2894.

Kolb G. 1977. The structure of the eye of *Pieris brassicae* L. (Lepidoptera). Zoomorph 87:123–146.

Kolb G. 1985. Ultrastructure and adaptation in the retina of *Aglais urticae* (Lepidoptera). Zoomorphology 105:90–98.

Kolb G. 1986. Retinal ultrastructure in the dorsal rim and large dorsal area of the eye of *Aglais urticae* (Lepidoptera). Zoomorphology 106:244–246.

Labhart T, Meyer EP. 1999. Detectors for polarized skylight in insects: a survey of ommatidial specializations in the dorsal rim area of the compound eye. Microsc Res Tech 47:368–379.

Maida TM. 1977. Microvillar orientation in the retina of a pierid butterfly. Z Naturforsch 32c:660–661.

Miller WH. 1979. Ocular optical filtering. In: Autrum H, editor. Handbook of sensory physiology. Volume VII/6A. Berlin: Springer-Verlag. p 69–143.

Miller WH, Bernard GD. 1968. Butterfly glow. J Ultrastruct Res 24:286–294.

Nilsson DE, Land MF, Howard J. 1988. Optics of the butterfly eye. J Comp Physiol A 162:341–366.

Peitsch DA, Fietz A, Hertel H, de Souza J, Ventura DF, Menzel R. 1992. The spectral input systems of hymenopteran insects and their receptor-based color vision. J Comp Physiol A 170:23–40.

Pepe, IM, Schwemer J, Paulsen R. 1982. Characteristics of retinal-binding proteins from the honey bee retina. Vis Res 22:775–781.

Qiu XD, Vanhoutte KAJ, Stavenga DG, Arikawa K. 2002. Ommatidial heterogeneity in the compound eye of the male small white butterfly, *Pieris rapae crucivora*. Cell Tissue Res 307:371–379.

Ribi WA. 1978. Ultrastructure and migration of screening pigments in the retina of *Pieris rapae* L. (Lepidoptera, Pieridae). Cell Tissue Res 191: 57–73.

Ribi WA. 1979. Structural differences in the tracheal tapetum of diurnal butterflies. Z Naturforsch 34c:284–287.

Ribi WA. 1987. Anatomical identification of spectral receptor types in the retina and lamina of the Australian orchard butterfly, *Papilio aegeus aegeus* D. Cell Tissue Res 247:393–407.

Sakamoto K, Hisatomi O, Tokunaga F, Eguchi E, 1996. Two opsins from the compound eye of the crab *Hemigrapsus sanguineus*. J Exp Biol 199:441–450.

Salcedo E, Huber A, Henrich S, Chadwell LV, Chou W-H, Paulsen R, Britt SG. 1999. Blue- and green-absorbing visual pigments of *Drosophila*: ectopic expression and physiological characterization of the R8 photoreceptor cell-specific Rh5 and Rh6 rhodopsins. J Neurosci 19:10716–10726.

Shimohigashi M, Tominaga Y. 1986. The compound eye of *Parnara guttata* (Insecta, Lepidoptera, Hesperiidae): fine structure of the ommatidium. Zoomorphology 106:131–136.

Silberglied RE. 1989. Visual communication and sexual selection among butterflies. In: Vane-Wright RI, Ackery PR, editors. The biology of butterflies. Princeton, NJ: Princeton University Press. p 207–221.

Smith WC, Goldsmith TH. 1991. The role of retinal isomerase in the visual cycle of the honeybee. J Gen Physiol 97:143–165.

Stavenga DG, Smits RP, Hoenders BJ. 1993. Simple exponential functions describing the absorbance bands of visual pigment spectra. Vis Res 33:1011–1017.

Stavenga DG, Hariyama T, Arikawa K. 2000. Spectral characteristics and regionalization of the eye of the satyrid *Bicyclus anynana*. Proc Exp Appl Entomol 11:77–82.

Stavenga DG, Kinoshita M, Yang EC, Arikawa K. 2001. Retinal regionalization and heterogeneity of butterfly eyes. Naturwissenschaften 88: 477–481.

Steiner A, Paul R, Gemperlein R. 1987. Retinal receptor types in *Aglais urticae* and *Pieris brassicae* (Lepidoptera), revealed by analysis of the electroretinogram obtained with Fourier interferometric stimulation (FIS). J Comp Physiol A 160:247–258.

Thompson JD, Higgins DG, Gibson TJ. 1994. Clustal W: improving the sensitivity of progressive multiple sequence alignment through sequence weighting, position-specific gap penalties and weight matrix choice. Nucleic Acids Res 22:4673–4680.

Townson SM, Chang BSW, Salcedo E, Chadwell LV, Pierce NE, Britt SG. 1998. Honeybee blue- and ultraviolet-sensitive opsins: cloning, heterologous expression in *Drosophila*, and physiological characterization. J Neurosci 18:2412–2422.

Weiss MR. 2001. Vision and learning in some neglected pollinators: beetles, flies, moths and butterflies. In: Chittka L, Thomson JD, editors. Cognitive ecology of pollination: animal behavior and floral evolution. Cambridge: Cambridge University Press. p 106–126.

White RH, Bennett RR. 1989. Ultrastructure of carotenoid deprivation in photoreceptors of *Manduca sexta*: myeloid bodies and intracellular microvilli. Cell Tissue Res 257:519–528.

APPENDIX
Computational model of reflectance spectrum for mixed ommatidia

A computational model was created under the following assumptions:

1. The measured eye region has a mixture of quantity N1 of type I ommatidia (six green and two UV rhabdomeres), N2 of type II ommatidia (six green, one blue, and one UV), and N3 of type III ommatidia (six green and two blue).
2. All three types contain the same amount of P530 (one-way integrated density = Dg).
3. Type I has no blue-absorbing visual pigment (Pblue), and type III has no P360.
4. Type II has the one-way integrated density (Duv) of the ultraviolet-absorbing visual pigment of R360 and the one-way integrated density (Db) of Pblue, of λmax to be determined.
5. Type I has 2*Duv of P360.
6. Type III has 2*Db of Pblue.
7. All three types have one-way integrated density (Dp) of a putative retinoid-binding protein, with λmax to be determined.
8. The distribution of these pigment mixtures, as a function of axial position along a rhabdom, is constant.
9. All three types have the same tapetum, approximated by the theoretical reflectance spectrum shown in Figure 4A.
10. If the rhabdoms are empty of these pigments, the measured reflectance spectrum is the same as the tapetal reflectance spectrum.
11. Only the first waveguide mode in each rhabdom is excited by measuring illumination.
12. The attenuation constant at any wavelength for the waveguide mode in a rhabdom is the cross-sectional average of the visual pigment mixture (Bernard, 1975). That attenuation constant does not change with axial position.

Procedure

1. Compute round-trip transmittance spectra for each ommatidial type then form a weighted average according to numbers N1, N2, and N3 of each ommatidial type present, multiplied by the tapetal reflectance spectrum, to model the experimental reflectance spectrum. The results from in situ hybridization indicated that the central portion of the ventral eye retina has relatively light distribution of P360 and heavier distribution of P470 (Fig. 7A,B). Suppose in the measured region, which is somewhat below center, that the 20 ommatidia contain equal numbers of UV and blue rhabdomeres (20 each), in which case N1 = 5, N2 = 10, and N3 = 5.
2. Adjust Dg of P530 so that, when stripped from the experimental reflectance spectrum, the computed spectrum fits the tapetal spectrum in the band between 550 and 600 nm, because none of the remaining pigments have significant absorbance in that band. Dg = 0.62 produces that fit.
3. Adjust Db and λmax of blue-absorbing visual pigment, so that, when stripped from the experimental spectrum, the computed spectrum fits the tapetal spectrum in the band between 450 and 550 nm because none of the remaining pigments have significant absorbance in that band. Db = 0.12 of R470 produces that fit.
4. Knowing that the UV visual pigment peaks at 360 nm (Chen, 1987) and expecting that Duv should be about the same as Db, stripping that amount produces a spectrum that has a residual rhodopsin-like dip in the neighborhood of 395 nm. Fix the λmax of that unknown pigment at 395 nm and determine densities Duv and Dp that best fit the tapetal spectrum. Duv = 0.15 and Dp = 0.11 produce that fit. The resultant spectrum, plotted with a black line in Figure 4A, closely approximates the theoretical reflectance spectrum of the tapetum (open squares, Fig. 4A).

One might think that a better computational model might be a conventional least-squares fit to a mixture of pigments, for which there are six free parameters to be determined (λmax and densities of all three visual pigments). That procedure assumes that the errors are uniformly distributed over wavelength, not valid in this situation. The successive stripping approach exploits the fact that the tapetum is white, turning a 6 degrees-of-freedom curve fit over the entire wavelength range into a successive series of 1 or 2 degrees-of-freedom fits over limited wavelength ranges.